Heat Conduction Mechanisms in Nanofluids and Suspensions

J. J. Wang, R. T. Zheng[1], J. W. Gao[2], and G. Chen[*]

Department of Mechanical Engineering, Massachusetts Institute of Technology, 77 Massachusetts Avenue, Cambridge, Massachusetts 02139, USA

KEYWORDS: Nanofluids; Graphite suspensions; Clustering; AC impedance spectroscopy; Thermal conductivity; Phase transition

1. Introduction

Nanofluids-colloids obtained by mixing nanoparticles with a base fluid-have attracted wide attention since Choi coined the term in 1995 and observed that they have much higher thermal conductivity than anticipated from the effective medium theories [1–7]. In fact, adding particles into a liquid to improve its thermal conductivity is an old idea. Researchers have tried to add micron sized or larger solid particles into liquids to increase their thermal conductivity, as solids usually have much higher thermal conductivity than liquids [8]. The thermal conductivity of these suspensions can be predicted by the effective medium theory which was originated from Maxwell [9] and continuously improved by many researchers to include factors such as interfacial

[1] Present address: College of Nuclear Science and Technology, Beijing Normal University, Beijing 100875, China
[2] Present address: School of Physics and Telecommunication Engineering, South China Normal University, Guangzhou 510631, China
[*] Corresponding author. Tel.: 617-253-0006;
Fax: 617-324-5519.
E-mail address: gchen2@mit.edu

thermal resistance between the particles and the base fluid, and shape of the particulates [10–13]. However, large particles are prone to settling out of the suspensions. There are also some other drawbacks that limit the applications of fluids loaded with large particles [8,14,15], as the particles are likely to: 1) clog the flow channel, 2) abrade the surface of fluid channel, and 3) increase the pressure drop. As an alternative, researchers drew the attention from using large particles to dispersing nanoparticles into the liquids. In fact, Masuda et al. [16] investigated the thermal conductivity and viscosity of suspensions containing alumina, silica, and titanium dioxide nanoparticles before Choi et al.'s studies [1]. Current interest towards nanofluids is fueled by both fundamental science and applications. On the fundamental side, mechanisms of heat conduction and enhanced thermal conductivity in nanofluids are of great interest [17–20]. On the application side, the enhanced thermal conductivity of nanofluids promises applications in thermal systems [21–23].

Since its interception, nanofluids have been a controversial topic. First, some previously reported high thermal conductivity cannot be repeated by others [24–27]. This has raised questions on the accuracy of the experimental method. However, a world-wide round-robin involving 33 laboratories has shown reasonable consistency in thermal conductivity measurement methods, especially the widely used transient hot-wire method, despite the fact that nanofluids studied by the round-robin groups did not show anomalous increase in thermal conductivity [28]. Second, many potential mechanisms have been proposed on why thermal conductivity can be increased beyond the effective medium theories, although careful reasoning can rule out most of them [18,29,30]. Fueled by these controversies, publications on nanofluids continue to increase, and many reviews are written.

The purposes of this article are to summarize our understanding of heat conduction

mechanisms in nanofluids, arising from our past work in this area [19,31–39] and our knowledge of other studies in this field. Due to the large number of existing reviews [3–7,40–43], we do not intend to give a systematic summary of past work in the literature. We will first discuss potential mechanisms that can affect heat conduction in nanofluids. Most of these mechanisms have already been discussed in literatures, but we bring in additional insights from our understanding of heat conduction in solids and liquids, and Brownian motion. Like several previous theoretical analysis [44–48], we believe clustering is the key mechanism for thermal conductivity enhancement. Our conclusion is mostly based on our own experimental observations. This understanding led us to develop graphite-flake based suspensions. The graphite flakes have several tens of nanometers in thickness, but several microns in lateral size. These suspensions fall in between nanofluids and microfluids, and can be made stable in oil as well as in water. Although there have already been reports that such suspensions can have much enhanced thermal conductivity [49–51], we will show new experimental observations, such as thermal percolation, and demonstrate reversible regulation of electrical and thermal conductivity of such suspensions going through liquid-solid phase change process in addition to achieving very high thermal conductivity values. We will conclude this paper by proposing a few interesting research directions arising from past work.

2. Heat conduction mechanisms in nanofluids

We will first summarize heat conduction mechanisms in solid, liquid, and solid-liquid interface, then move on to elaborate on potential mechanisms that can affect heat conduction in nanofluids.

2.1 Heat conduction mechanisms in solids, liquids, and liquid-solid interfaces

2.1.1 Heat conduction in solids. Most heat in crystalline dielectric and semiconductors is carried by phonons which are quantized lattice vibrations [52]. At or above room temperature, the thermal conductivity of bulk crystalline solids usually decreases with increasing temperature. Phonons in crystalline solids have a wide range of mean free paths. According to kinetic theory, the thermal conductivity can be expressed as

$$k = \frac{1}{3}\int C(\omega)v(\omega)\Lambda(\omega)d\omega = \frac{1}{3}Cv\Lambda \qquad (1)$$

where C is the specific heat per unit volume, v the phonon group velocity, and Λ the mean free path. The first equality emphasizes that these quantities all depend on the frequency of the phonon vibration in the solid, while the second equality is often used to estimate the phonon mean free path based on measured thermal conductivity values, specific heat and the speed of sound. Due to the neglect of the frequency dependence, the latter equality can cause large errors. In Si, for example, phonons with a mean free path less than 10 nm, 100 nm, and 1 μm contribute about 1%, 30%, and 60% respectively to the total thermal conductivity of 136 W/mK, according to first principle simulations at room temperature [53,54], while the second equality will give a phonon mean free path of only 40 nm. At or above room temperature, the thermal conductivity of bulk crystalline solids usually decreases with increasing temperature, because at high temperatures, the mean free path decreases with increasing temperatures due to phonon-phonon scatterings. In amorphous solids, the phonon picture is less valid due to lack of periodicity in the arrangement of atoms. Thermal conductivity near room temperature in amorphous solids roughly follow the trend of specific heat (i.e., slowly

increases with temperature to saturation), due to the short lifetime of vibrational modes. Roughly, the phonon mean free path in Eq. (1) is the same order as atomic separations. In metals, electrons dominate the heat conduction, and Eq. (1) applies if each quantity represents that of electrons. The mean free paths of electrons in metals are usually very short, on the order of a few nanometers [55]. The thermal conductivity of metals typically decreases with increasing temperature due to increased scattering of electrons at higher temperatures.

The thermal conductivity of individual nanoparticles is difficult to measure. However, it is anticipated that as the diameter of nanoparticles becomes comparable to the phonon or electron's mean free path in bulk materials, the distance that these carriers can travel are limited to roughly the diameter of the nanoparticle. Hence, the temperature dependence of thermal conductivity of very small nanoparticles should be similar to that of their specific heat, i.e., slowly increases with increasing temperature and eventually saturates at higher temperatures. As the nanoparticle diameter decreases, their thermal conductivity can either increase with increasing temperature or still decrease with increasing temperature as in bulk crystalline solids. Other nanostructures such as carbon nanotubes and graphenes can have higher thermal conductivity than bulk graphite because they are closer to one-dimensional or two-dimensional systems, which can have less scattering than bulk structures [56–58]. However, it is not clear how the liquid environment would affect the scattering within graphenes or carbon nanotubes. Past experimental data show that isolated carbon nanotubes or graphenes can have thermal conductivity either increasing or decreasing with increasing temperature near room temperature [56,59]. This signifies the competition between boundary scattering (some from surface defects and others from the end effects) and internal phonon-phonon scattering.

2.1.2 Heat conduction in liquids. The picture of heat conduction mechanisms in liquids is more complicated than that in solids. Heat conduction can be mediated by translational, vibrational, and rotational modes of the molecules composing the liquid and conduction within the molecules themselves, especially in organic liquids with long molecular chains [60]. In most liquids, thermal conductivity increases as temperature decreases, while the opposite trend is observed in water [61,62].

2.1.3 Heat transfer through liquid-solid interface. Thermal boundary resistance exists at solid-solid and solid-liquid interfaces even if they are in perfect contact [52]. Although most studies on thermal boundary resistance is focused on solid-solid interfaces, thermal boundary resistance [63,64], also called Kapitza resistance, was actually first observed between liquid helium and a solid [65]. Mechanisms for the additional resistance at the interfaces are mismatch in the characteristics of the heat carriers on the two sides [66,67]. In the case of dielectric-dielectric interfaces, the mismatch in the atomic potential and mass leads to reflection of phonons. Transmission of energy modes across interfaces, however, depends on details of interfacial structures. Even to now, there exists no good model that can accurately predict thermal interfacial resistance. There are less liquid-solid interfacial resistance data [68–71], especially the temperature dependence of liquid-solid interfacial resistance. Cahill et al. [70] measured interfacial thermal conductance of carbon nanotubes suspended in surfactant micelles in water to be around $12\,\mathrm{MW\,m^{-2}K^{-1}}$. Schmidt et al. [34] also measured the effect of surfactants on the interfacial thermal conductance. These measurements show that the typical values of interfacial thermal conductance vary from several tens to several hundreds $\mathrm{MW\,m^{-2}K^{-1}}$. Such thermal conductance value is equivalent to a several tens

to several hundreds nanometers layer of solid with a thermal conductivity of 10 W/m-K. Despite the lack of experimental data, we expect that interfacial thermal resistance between liquid and solid will decrease with increasing temperature, similar to the specific heat behavior.

2.2 Potential mechanisms affecting heat conduction in nanofluids

Possible heat conduction mechanisms in nanofluids have been discussed in different literatures [3,5,18,40]. These include (1) Brownian motion of nanoparticles, (2) clustering of nanoparticles, (3) nanolayering of the liquid at the liquid/nanoparticle interface, (4) ballistic transport and nonlocal effect, (5) thermophoretic effect, and (6) near-field radiation. Many models have been developed for each or combinations of these mechanisms. In numerous publications, these models were shown to be capable of fitting experimental data. Although the ability to fit experimental data enhances credibility of models, the fact that models based on different mechanisms can explain same or similar data do not help understand the mechanisms. Detailed investigations would reveal that fitting parameters are often not physical.

2.2.1 Brownian motion. Different views on the importance of Brownian motion for thermal conductivity enhancement has been discussed in many literatures [18],[72,73]. Einstein developed basic theory for Brownian motion [74] and arrived at the basic relationship between diffusivity a of a particle in a fluid of viscosity μ

$$a = \frac{k_B T}{3\pi d \mu} \qquad \textbf{(2)}$$

where d is the particle diameter, and k_B the Boltzmann constant.

A formal theory for Brownian motion usually starts from the Langevin equation that governs the instantaneous velocity of the Brownian particle and can be written as

$$m\frac{d\mathbf{v}}{dt} = -m\eta\mathbf{v} + \mathbf{R}(t) \tag{3}$$

where m is the Brownian particle, $\mathbf{R}(t)$ is the random driving force, and η is the friction coefficient. For a spherical Brownian particle in a fluid, the Stokes law gives $\eta=3\pi d\mu/m$. Solution of the Langevin equation shows that the velocity of the Brownian particle decays exponentially with a time constant,

$$\tau = \frac{1}{\eta} = \frac{m}{3\pi d\mu} = \frac{\rho d^2}{18\mu} \tag{4}$$

The average velocity of the Brownian particle is given by

$$\mathrm{v} = \sqrt{\frac{3k_B T}{m}} \tag{5}$$

Using the above relations, one can quickly estimate the maximum potential contribution from the Brownian motion. Under the kinetic expression of Eq.(1), despite its inadequacy for liquid environment, the thermal conductivity contribution of Brownian particles is proportional to

$$\mathrm{k}_{\mathrm{Brownian}} = \frac{1}{3}\mathrm{Cv}\Lambda = \frac{1}{3}\mathrm{Cv}^2\tau = \frac{k_B TC}{3\pi d\mu} \tag{6}$$

By the same argument, one can also apply the above expression for the liquid itself, and the ratio of the Brownian particles' contribution to thermal conductivity to the thermal conductivity of base fluid is

$$\frac{\mathrm{k}_{\mathrm{Brownian}}}{\mathrm{k}_{\mathrm{bf}}} == \frac{(C/d)_{\mathrm{np}}}{(C/d)_{\mathrm{bf}}} \tag{7}$$

where the subscripts bf and np are base fluid and nanoparticles, respectively. As the

base fluid molecular diameter is usually two orders of magnitude smaller than that of the nanoparticle, the above expression shows that Brownian motion contribution to the thermal conductivity is at least two orders of magnitude smaller than that of the base fluid, even if we take the specific heat per unit volume of the nanoparticles equal to that of the base fluid, assuming that the Brownian motion of nanoparticles causes the surrounding fluid molecules to move at the same pace. If only the specific heat of the nanoparticles is used, the thermal conductivity ratio in Eq.(7) is further reduced by the volume fraction of the nanoparticles. Thus, existing models based on the pure motion of the nanoparticles are questionable. Keblinski and Cahill [75] pointed this out early in the debate on the role of Brownian motion.

Another opposite argument supporting the importance of Brownian motion is the microconvection argument. Convective heat transfer coefficient expressions between a heated sphere and cold surrounding fluid have been used to explain nanofluid's thermal conductivity enhancements with reasonable fit to experimental data [72,73], assuming surrounding fluid velocity equal the average thermal velocity of the Brownian particles. These models lack a physical picture to connect heat conduction through liquids and nanoparticles to that of heat transfer away from a heated nanoparticle maintained at a constant temperature.

Pure kinetic motion based models neglected potential interactions among nanoparticles. Bhattacharya et al. [76] considered potential interactions of nanoparticles, starting from the Langevin equation and using the Green-Kubo formulation. Although this is an interesting theoretical approach, careful examination of the parameters used in the potential suggests that these parameters are way too strong than in any nanofluids. The senior author of this paper had considered an electrothermal effect that includes the long range energy exchange between nanoparticles through electrical double layer

surrounding nanoparticles and random Brownian motion of the nanoparticles [77]. Although the theoretically treatment was interesting and expressions were correct, an error occurred in numerical substitution that leads to wrong the conclusion that electrothermal effect was important. Correct numerical calculations show that this effect is too weak to explain experimental data. We conclude that potential interactions among Brownian motion of nanoparticles are unable to explain the experimental observations.

There remains one important point in the Brownian motion picture that has not been fully understood. Langevin equation as given by Eq. (3) assumes steady state motion of the nanoparticle and hence the drag on the nanoparticle. Including the transient effect of the Stokes flow will lead to a memory effect – an integral Langevin equation. The solution of such an equation shows that velocity decay follows a power law rather than exponential function, as originally discovered by computational simulation [78]. The power law decay is much slower than the exponential decay, and this fact has been used as the basis to develop a kinetic argument by Xuan Yimin [79] and Bao Yang [80]. However, rigorous solutions of the retarded Langevin equation shows that the Einstein relation, Eq.(2), although obtained under the exponential decay solution of velocity, still holds true. This fact casts doubts on the power-law based kinetic picture. Molecular dynamics simulation further shows that the hydrodynamic effect caused by Brownian motion cannot provide an answer for the increased thermal conductivity [26,81].

Some experimentally reported temperature dependence of the thermal conductivity shows faster increase with increasing temperature than that of the base fluids [82], although opposite behavior or no change have also been reported in other nanofluids [27,83]. The former behavior is often used to support the claim on the importance of Brownian motion. However, as discussed before, size effects on the thermal

conductivity of crystalline nanoparticles, as well as the thermal boundary resistances all can contribute to increasing thermal conductivity with increasing temperature.

2.2.2 Clustering. Although the simplest picture of nanofluids is that nanoparticles are isolated and uniformly dispersed in the liquid, real suspensions of nanoparticles in liquids are more complicated. Nanoparticles themselves can interact, aggregate, and form internal structures [84–86]. The study of the states of the nanoparticles in a liquid falls into the realm of soft materials, which is a big branch of condensed matter physics. The internal structures of nanofluids can potentially explain the experimental results. In fact, our own experiments convinced us that the experimentally observed heat conduction behavior is mainly due to different states of the nanoparticles in the liquid, as we will discuss in detail later. The idea that nanoparticles form clusters and the formation of these clusters can explain the experimental results was discussed in a few papers [44–48]. Prasher et al. [44] started with the idea that clustered nanoparticles, which has a larger effective volume, together with their Brownian motion, can explain the experimental data, and then moved on to develop a three level homogenization model based on the effective media theory not involving Brownian motion, and suggested that such models can explain the experimental data.

2.2.3 Liquid layering. Near a solid surface, liquids are structured due to the influence of the potential of the solids, creating a crystalline layer typically 1-5 atomic layers (~1 nm) [43]. Crystal structures should have higher thermal conductivity than liquids. This mechanism is sometimes cited as potentially responsible for the increased thermal conductivity of nanofluids. However, as analyzed by Keblinski et al. [30], the liquid layering unlikely will be able to explain experimental observations. Furthermore,

due to phonon size effects in solids, 1-5 atomic layer crystal films will have significantly reduced thermal conductivity compared to their crystalline bulk materials, which further diminishes the likelihood that liquid layering can be a plausible cause.

2.2.4 Ballistic transport and nonlocal effects. Ballistic transport happens when internal scattering mechanisms are not strong enough, such that boundary and interfacial scattering becomes dominant [52]. Nonlocal heat conduction happens when ballistic transport occurs. Examples of ballistic transport are reduced thermal conductivity in solid nanostructures as we discussed before. Another example is nonlocal transport outside a nanostructure, which happens when the heat carrier mean free path in the surrounding media is much longer than the characteristic length of the nanostructure itself [87,88]. For both ballistic and nonlocal transport processes, the expectation is that heat transfer will be less than that predicted by the diffusion theory based on properties of bulk materials. Hence, it is unlikely that these effects have anything to do with experimental observation of anomalous thermal conductivity enhancements in nanofluids. A kinetic theory type model considering ballistic transport of nanoparticles in the liquid was proposed by Das [89]. However, to explain the experimental data, the mean free path of the solid nanoparticles in liquid would have to be in the range of centimeter, which is clearly out of the question [75].

2.2.5 Thermophoresis. Thermophoresis describes the movement of nanoparticles under a temperature gradient. On the higher temperature side, particles are subject to the bombardment of higher energy molecules, experiences higher force, and hence will be driven to the lower temperature side. This effect may affect the thermal conductivity measurements [90]. However, when we change the hot-wire temperature in

the experiment, and hence the temperature gradient, we did not observe any appreciable change in measured thermal conductivity, suggesting thermophoresis is not important. Analysis by Koo and Kleinstreuer also showed thermophoresis is not important to the thermal conductivity enhancements [91].

2.2.6 Near-field Radiation. Molecular dynamics simulation by Volz and co-authors showed that heat transfer between two nanoparticles increases rapidly as they get together [92]. Hence, it was suggested that near-field radiation may be a cause for increased thermal conductivity. Even though experiments have demonstrated that near-field radiation can be significantly higher than maximum radiation exchange described by blackbodies [93], radiation effect is always much smaller than heat conduction through a medium. Of course, as two surfaces are nearly in contact, the distinction between radiation and conduction diminishes. In the case of completely touching surfaces, our previous discussion on thermal boundary resistance between surfaces should apply. Hence, we do not believe that near-field radiation can explain the experimental data.

3. Summary of our experimental work

The senior author's group has been working on nanofluids over the past few years, mostly based on experiments [19,32,33,36,94]. We first verified that the transient hot-wire method and an optical technique give consistent results on thermal conductivity of nanofluids [36], establishing confidence on the hot-wire method. We started with Al_2O_3 nanoparticles dispersed in various fluids, including studying the effects of surfactants [34,37]. Experimental results, however, did not lead to anomalous thermal conductivity enhancements, although experimental data could be slightly above the model predictions based on isolated spherical particles. Copper nanoparticle based

nanofludis were also studied, with similar results [32]. In several nanofluids, a reduction in thermal conductivity was also observed.

Our revelation of potential heat conduction mechanisms came from freezing experiments. If Brownian motion is the culprit for enhanced thermal conductivity, we expect to see that the same suspension, when freezes, should have a lower thermal conductivity enhancement. Gao et al. [19] carried out freezing experiments on alumina nanofluids using two different host materials: animal oil and hexadecane. For the animal oil based nanofluids, the thermal conductivity enhancement was slightly lower in the solid state than the liquid state. For the hexadecane based nanofluids, however, the solid state had an even higher thermal conductivity enhancement than the liquid state. Transmission electron microscope (TEM) images (Fig.1) show that Al_2O_3 nanoparticles chain up when hexadecane freezes and forms crystals, but this phenomenon does not happen when the animal oil freezes. This is because when hexadecane freezes, it forms crystals and Al_2O_3 nanoparticles are pushed into the grain boundaries between the crystallites. This experiment suggests that nanoparticle clustering into chains and forming a percolation network will help improve the thermal conductivity because in this case, heat prefers to conduct along the clusters that are composed of higher thermal conductivity nanoparticles.

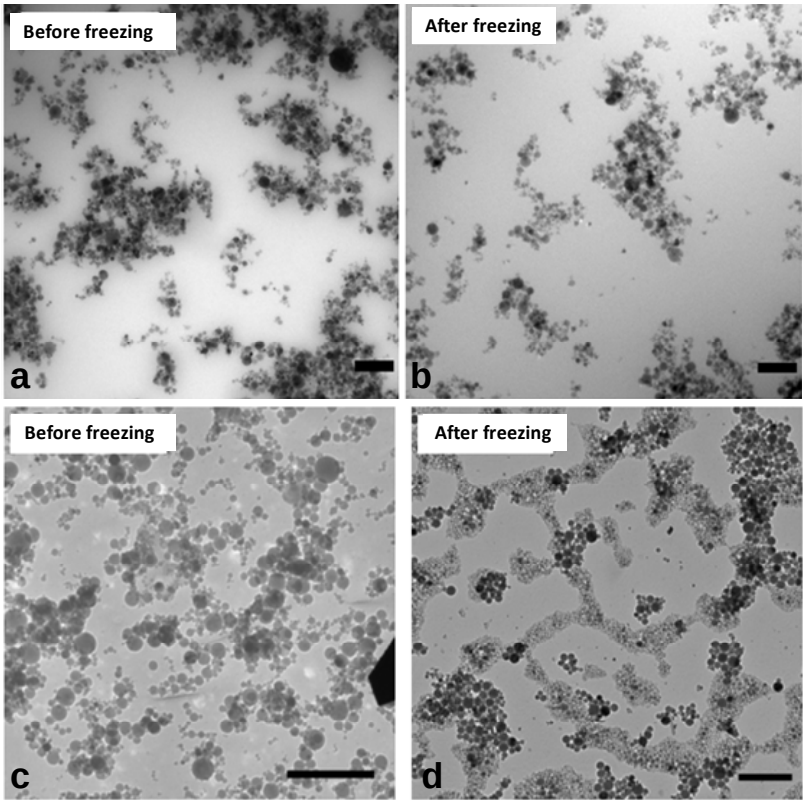

Figure 1: TEM image of alumina (a) in hog fat suspension before freezing, (b) in hog fat composite after freezing, (c) in hexadecane suspension before freezing, (d) in hexadecane composite after freezing.

From [19].

If conduction along the backbones of nanoparticles is responsible for thermal conductivity improvements, then nanoparticles are not the best choices because 1) nanoparticles usually have low thermal conductivity due to size effects discussed before, and 2) interfacial resistance between nanoparticles limit heat conduction along the nanoparticle chains. Large anisotropic particulates such as graphite flakes or carbon nanotubes are better choices. We choose graphite flakes as additives because graphite flakes have very high in-plane thermal conductivity, are low cost, and may form clusters. It is envisioned that the thermal boundary resistance between graphite flakes is likely to be bad for heat conduction along the clusters. To reduce the thermal boundary

resistance, graphite flakes should be made into larger particles as long as stable suspensions can be formed. There may also be an optimal thickness as thermal conductivity of too thin flakes may be low due to phonon scattering by the surrounding fluid molecules, and too thick flakes will require large amount of materials for the percolation network to form and also the suspension may have stability problem. However, the optimal thickness is still under study

The greatest challenge of making nanofluids is stability. When the nanoparticles are lyophobic to the base fluids, it is very hard to prepare stable nanofluids since the particles "hate" to contact with the liquid and try to separate from it. In this case, surfactants (molecules usually consisting of a long lyophobic "tail" and a lyophilic "head") are frequently used to wrap the nanoparticles to improve the lyophilicity of the particle phase and consequently increase the stability. However, the presence of surfactants increases the interfacial resistance between the nanoparticles and base fluids, and therefore will reduce the thermal conductivity enhancement of nanofluids if the heat conduction is primarily along the nanoparticles.

The preparation of our graphite suspensions is a two-step process. The first step is to produce graphite particles. Natural graphite particles are large-sized and too thick, which cannot be directly mixed with the base fluid, as large particles will settle out very quickly. To avoid this, we use chemical intercalation [95–99] and microwave expansion to obtain exfoliated graphite flakes, followed by an ultrasonic process to disperse the flakes into the liquid. For example, 85 ml of H_2SO4 (96%) and 15 ml of hydrogen peroxide (30%) were mixed to form an oxidative agent that was used for the intercalation. For the intercalation process, 2.2 g of natural graphite was reacted with

100 ml of the oxidative agent at room temperature for 60 min. The slurries were rinsed with distilled water to remove residual salts and acids, followed by filtering and baking on a hotplate at 110ºC for 24 hours. The expanded graphite was obtained by thermal expansion of as-prepared graphite intercalation compounds in a 1100W commercial microwave oven for 5~30s. The expanded graphite was then dispersed in ethylene glycol and other liquids to create graphite suspension using a high intensity ultrasonic probe. The samples were sonicated from 3-30 minutes, depends on the volume fraction of graphite flakes.

The microwave expansion is a rapid heating process which creates pressure between graphite layers and thus significantly expands the interlayer spacing. However, too long microwave time (e.g. longer than 30 seconds) should be avoided since heating will anneal most of the surface functional groups introduced during the chemical intercalation process. Natural graphite is lyophilic to ethylene glycol and PAO but lyophobic to DI water. However, because of the introduction of surface functional groups, the wettability of the graphite flake changes. We carried out C1s X-ray photoelectron spectra on the exfoliated graphite flakes and found *C*=*C*, *C*−*OH*, *C*=*O* and *O*=C−*OH* species [33]. The polar groups increase hydrophilicity of the flakes. We were able to create stable suspensions using de-ionized water (DI water), ethylene glycol, and poly-alpha-olefin (PAO), and hexadecane. To make the expanded graphite disperse uniformly in the base fluids, we must use an ultrasonic probe to sonicate the mixture. The sonication time varies as the graphite volume fraction increases. We observed that too short sonication time will make the samples too viscous, especially at high volume fractions, while too long sonication time can substantially reduce the viscousity but lessen the thermal conductivity enhancement of suspensions. Therefore,

there is a tradeoff between high thermal conductivity and low viscosity. Figures 2(a) and (b) show the SEM and TEM images of graphite flakes after sonication. The graphite flakes have an average diameter of several microns and thickness from several to several tens of nanometers. Figure 2(c) shows measured thermal conductivity of PAO based graphite suspensions at three different microwave times.

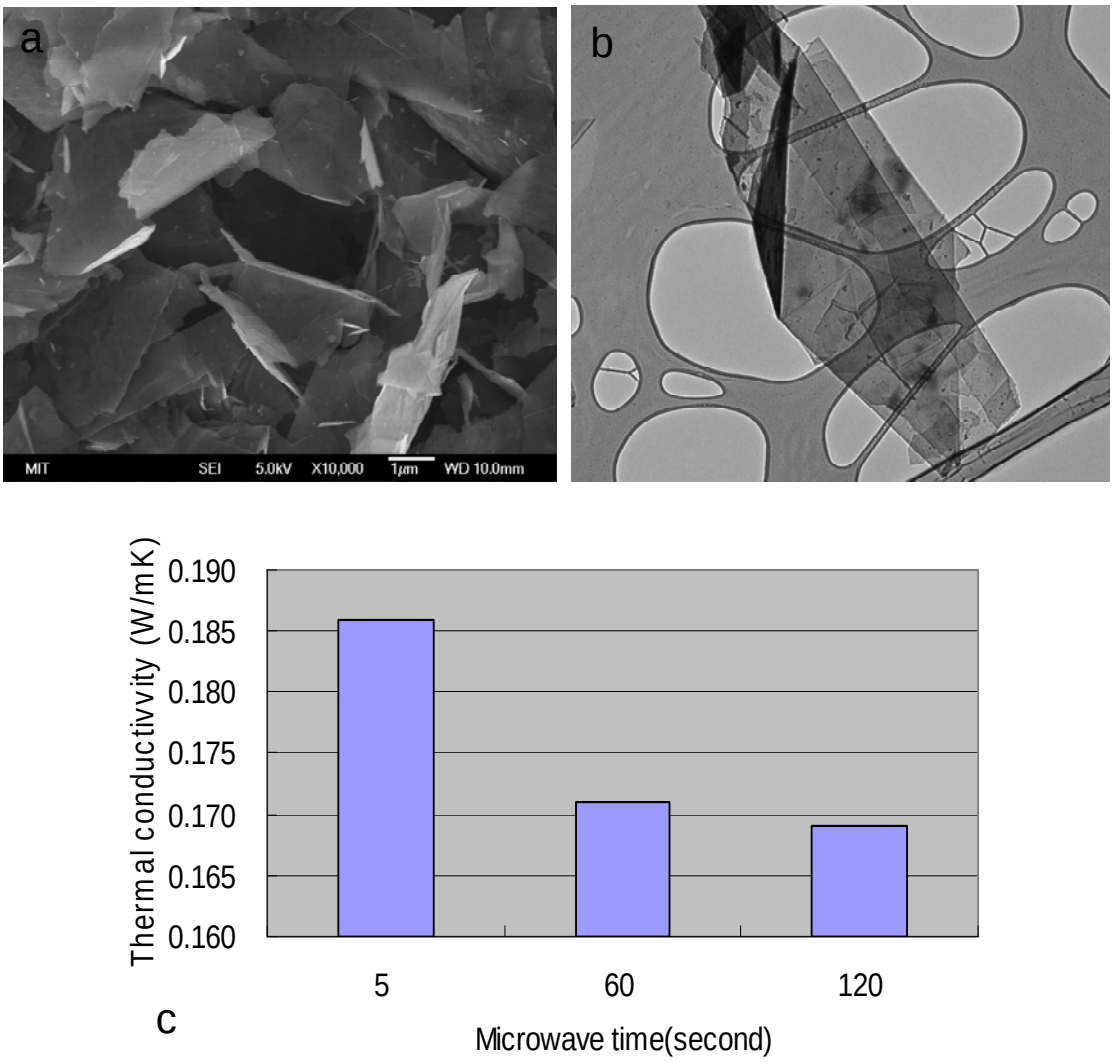

Figure 2: (a) SEM image of graphite flakes after sonication. (b) TEM image of graphite flakes after sonication. From [33]. (c) Thermal conductivity of PAO/graphite suspension (1% volume fraction) at three different microwave times (5 seconds, 60 seconds, 120 seconds).

Figure 3 shows the thermal conductivity enhancement as a function of graphite volume

fraction in three different base fluids (DI water, ethylene glycol, PAO) [100]. The addition of graphite particles to the base fluid increases the fluid's thermal conductivity dramatically and the enhancement increases as the graphite volume fraction increases. Shikh et al. [49] reported a 161% thermal conductivity enhancement of graphite nanofluids based on PAO at a volume fraction of 1%. Choi et al. [101] reported the same thermal conductivity enhancement while using carbon nanotubes in oil. For water-base graphite nanofluids, Zhu et al. [102] reported only a 12% thermal conductivity enhancement at a volume fraction of 1%, and Assael et al. [50] reported a 38% thermal conductivity enhancement. The thermal conductivity enhancements of the three kinds of graphite suspensions we made (201% for PAO, 153% for ethylene glycol, 113% for water) all exceed the maximum values reported in the literatures.

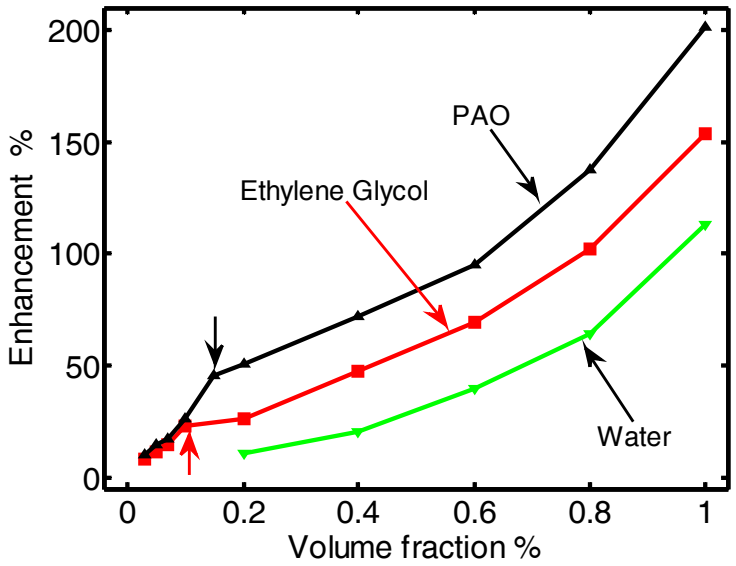

Figure 3: The thermal conductivity enhancement of three kinds of graphite suspensions as a function of volume fraction.

As stated before, the sonication time for different volume fractions is different. The higher the volume fraction, the longer the sonication time required. To investigate the effect of sonication time on the thermal conductivity enhancement, we test the thermal

conductivity enhancement of three kinds of graphite suspensions at the same volume fraction (1%), but prepared using different sonication times. Figure 4 shows the measurement results. It is obvious that too long sonication time will significantly reduce the thermal conductivity enhancement. This is because the high power of ultrasonication can break large particles into small pieces, which will generate more particle contacts, and thus increase the thermal contact resistance and decrease the thermal conductivity enhancement (see insets of figure 4). On the other hand, smaller particles do not settle out easily, which is help form stable suspensions. Since the sonication time has substantial effect on the suspension thermal conductivity, it is necessary to measure several sets of samples using the same sonication time. We sonicate at the highest volume fraction and dilute the sample to get lower volume fraction samples.

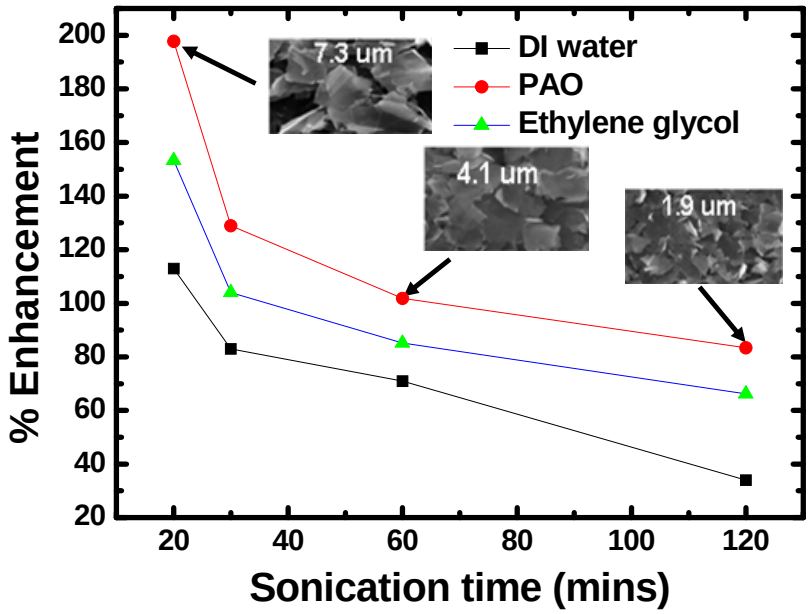

Figure 4: Thermal conductivity enhancement as a function of sonication time. All three kinds of graphite suspensions are 1% volume fraction. The insets are three SEM images of graphite flakes after sonicating 20 mins, 60 mins, and 120 mins with average flake diameter 7.3 μm, 4.1 μm, and 1.9 μm, respectively, based on the statistics from SEM image.

Graphite suspensions at low volume fractions (lower than 0.2%), especially for the water-based graphite suspensions, are less stable than that at high volume fractions (higher than 0.2%). At low volume fractions, graphite particles can only form isolated clusters. At high volume fractions, the previously isolated clusters can connect with each other to form percolated structure. This percolated structure provides a strong support for the graphite flakes so that they will not settle out for a long time.

For ethylene glycol and PAO curves (Fig. 3), we see two extraordinary features in the volume fraction dependence of thermal conductivity enhancement. First, there is a sharp kink in the thermal conductivity dependence on the volume fraction. At the kink point, the thermal conductivity value is continuous but the slope changes sharply. Second, below the kink point, thermal conductivity increases more rapidly with volume fraction than above the kink point. This is opposite from the electrical conductivity, which increases rapidly after the electrical percolation. The kink in thermal conductivity may be related to percolation. However, it is well-known that percolation does not lead to sharp transitions in the thermal conductivity because heat conduction can occur in both liquid phase and solid phase, which smoothes out the thermal percolation transition [103,104]. Further more, it is generally expected that after the onset of percolation, the thermal conductivity increase rate will be much higher, which contradicts our experimental observations.

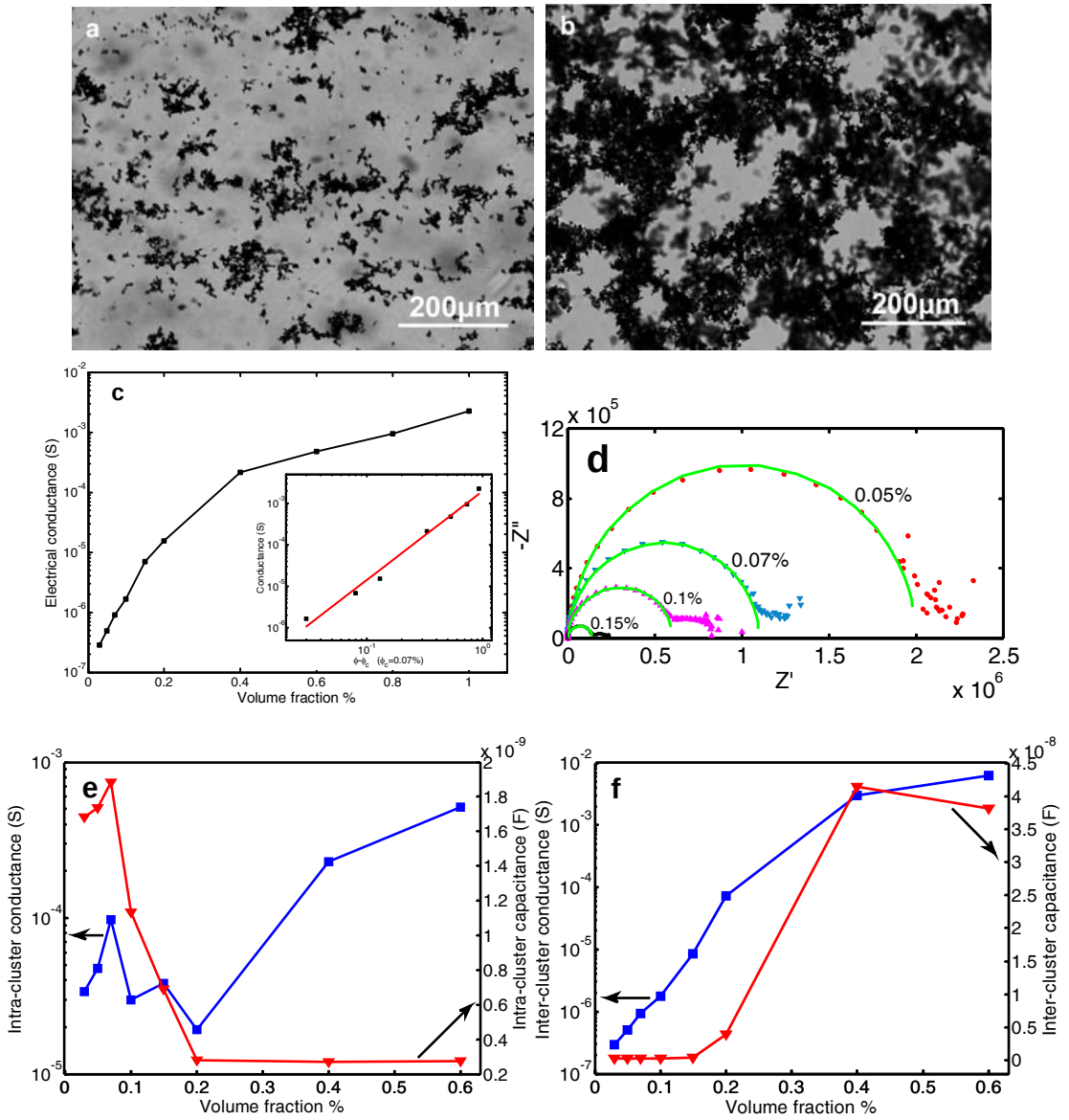

Figure 5: Optical images of the microstructures of EG-based graphite suspensions at different volume fractions: (a) 0.03% and (b) 0.1% . (c) Electrical conductance shows a percolation behavior at 0.07% for 25 minutes ultrasonic time. (d) Nyquist plots of AC impedance of EG/graphite suspensions at different volume loadings. (e) Intra-cluster and (f) inter-cluster resistance and capacitance as a function of graphite volume fraction.

From [100].

We combined optical microscopy with AC impedance spectroscopy to understand the extraordinary features observed [100]. Optical images of graphite suspensions show that

at low volume fractions, the graphite flakes form isolated clusters and the suspension is more solution-like. At high volume fractions, the graphite clusters merge into percolation structures and the suspension is more gel-like. Electrical conductance measurements show a percolation threshold at 0.07% volume fraction, consistent with the kink location in the thermal conductivity.

Based on the microstructural evolution (Fig. 5a and 5b) and AC impedance spectroscopy (Fig. 5c-5f) studies, the sharp inflection in thermal conductivity can be explained as follows. Below the percolation threshold, graphite flakes form clusters. These clusters tend to minimize the surface energy via tighter binding among the graphite flakes. As the clusters merge to form a percolation network, the driving force to minimize surface energy becomes smaller, and the binding between graphite flakes becomes weaker and graphite flake separation increases, which leads to decreased flake-to-flake (intra-cluster) conductance and decreased capacitance (Fig. 5e) but an increased inter-cluster conductance (Fig.5f). As the flake-flake separation increases within the cluster, thermal interface resistance between graphite flakes increases, leading to a slower rate of increase at high volume fractions.

Our experiments also provide insights into the conflicting experimental results in the nanofluids field [18,28,105]. Most previous experimental data on spherical nanoparticles have not reached the percolation phase transition point and transport lies in either the isolated particle or the isolated cluster regime. A similar kink behavior can be seen in the thermal conductivity data of CuO nanofluids, although the paper does not discuss this behavior [45]. High aspect ratio nanoparticles, such as carbon nanotubes based nanofluids, have lower percolation thresholds, and past experiments were already in the

percolated regime. We should emphasize that thermal conductivity depends strongly on how the suspensions are prepared, reflecting the fact that states of the particulates in liquids are very complicated [84–86]. In Fig. 6, we show thermal conductivity of suspensions of graphite in ethylene glycol, prepared using various sonication times. The complex trend of thermal conductivity testifies to the difficulties in repeating data from different groups, as varying the sonication time not only changes the mixing but also the size of the graphite flakes. For this reason, we spent a long time repeating data presented in Fig. 3, and obtained consistency by first preparing samples at higher volume concentration, followed by dilution with magnetic stirring.

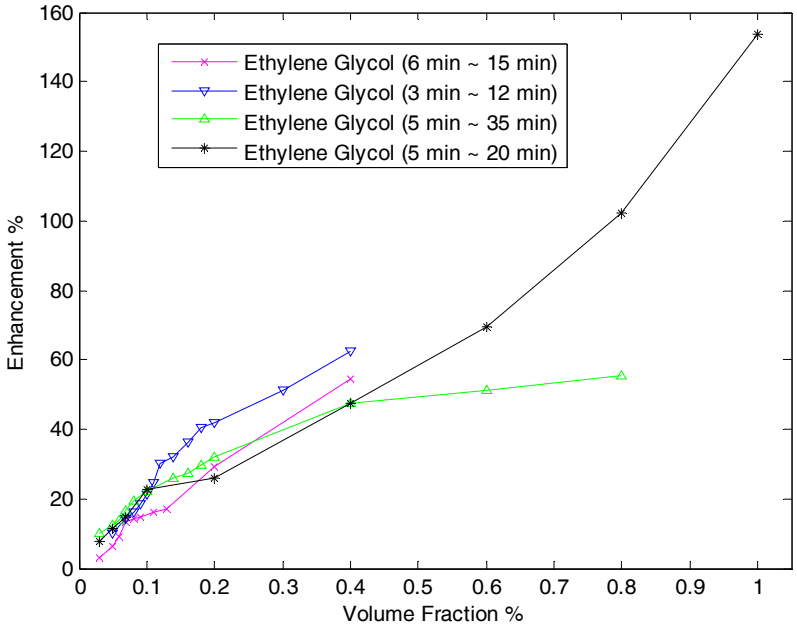

Figure 6: Several sets of data on the thermal conductivity enhancement of ethylene glycol based graphite suspensions. These sets of suspensions samples were prepared by the same method but using different sonication times. Generally, higher volume fraction samples were prepared using longer sonication time; lower volume fraction samples were prepared using shorter sonication time. For the same volume fraction samples, we adjusted the sonication time to control the thermal conductivity to be a little higher or lower.

Our understanding is also instructive for achieving high thermal conductivities in dilute suspensions. First, thermal conductivity enhancement is due to heat conduction within the solid, and hence high thermal conductivity additives should be used. Second, high thermal conductivity additives that easily form clusters will not only help to stabilize suspensions, but also enhance the thermal conductivity at low volume fractions. Third, high interface density in the suspensions will effectively suppress the thermal conductivity enhancement because the interface thermal resistance is detrimental to thermal transport. Hence, particulates with high aspect ratios (such as carbon nanotubes and graphite flakes), by forming tightly-bonded clusters and suppressing the interface resistance, can become excellent additives to achieve high thermal conductivity.

4. Reversible temperature regulation of suspension properties

Our freezing experiment on Al_2O_3 nanoparticles in crystalline forming liquid led us to perform similar experiments on graphite suspensions [33]. We choose to use hexadecane as the matrix. This is because the phase transition temperature of hexadecane is around $18\,°C$, which is convenient for experimentation. We prepared the hexadecane based graphite composites and measured both electrical conductivity and thermal conductivity in the solid state and the liquid state. Cyclic measurements on the electrical conductivity and the thermal conductivity were performed to test their reversibility. Figure 7(a) shows the cyclic behavior of the electrical conductivity as the suspension goes through repeated melting and freezing processes. The first freezing cycle shows the largest electrical conductivity contrast because it contains more loose clusters in the liquid state. In the first remelting process, contacts between graphite flakes degrade dramatically, leading to a sharp reduction in electrical conductivity. However, many graphite flakes will be trapped in the percolation network and so the electrical

conductivity in the liquid state increases from its original synthesized state. After the first cycle, the percolation structure becomes stable and the electrical conductivity contrast of graphite composites approaches a constant. Figure 7(b) shows the cyclic behavior of the thermal conductivity as the suspension goes through repeated melting and freezing processes.

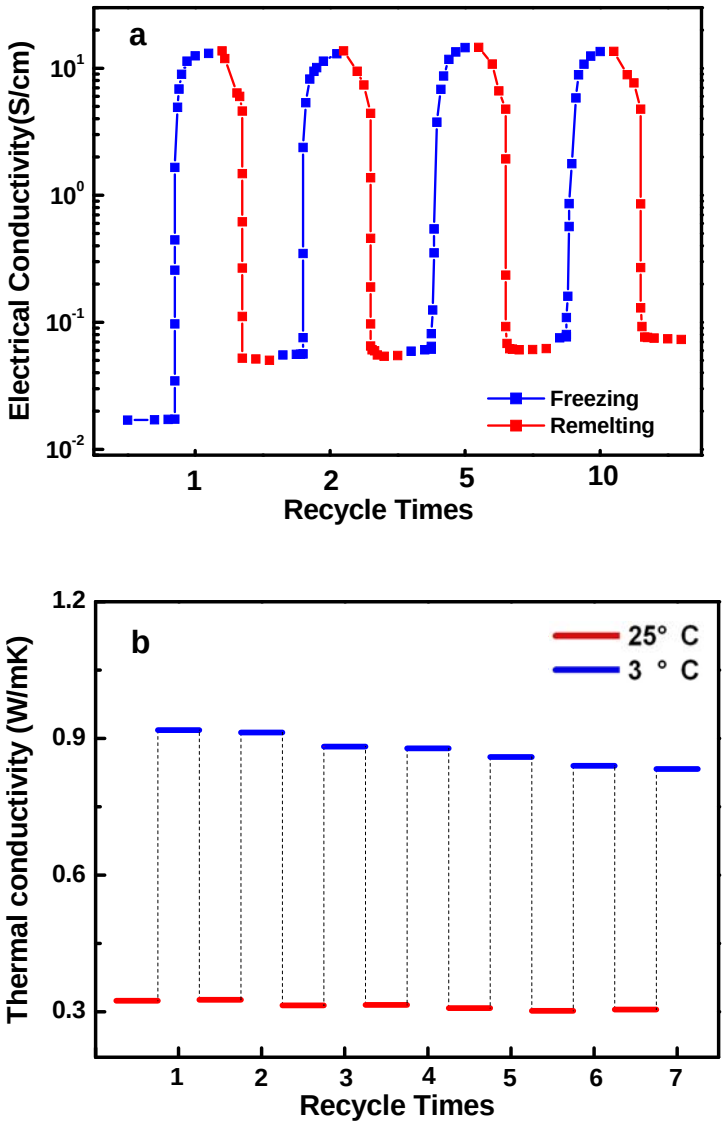

Figure 7: (a) Electrical conductivity contrast after different cycles. Blue lines indicate the electrical conductivity of 0.8% hexadecane based graphite composites in the course of freezing, while red lines indicate that in the course of melting. (b) Thermal conductivity contrast after different cycles. Blue lines indicate the thermal conductivity of 0.8% hexadecane based graphite composites at 3°C

during different cycles, while red lines indicate that at 25°C during different cycles.

From [33].

The significant electrical and thermal conductivity contrast between solid state and liquid state can be explained as follows. During freezing, the graphite particles are squeezed to the grain boundaries [106–108]. The internal stress generated during freezing regulates contacts among particles, increasing the thermal conductivity of the sample. In the liquid state, the contact among graphite particles is loose and weak. Hence the interfacial thermal resistance between two flakes is high, and the total thermal conductivity of the suspension is small. During the freezing of the hexadecane, needle-like structures are formed. The anisotropic growth of the hexadecane crystals generates pressure, rapidly increasing the contact area of graphite flakes, reducing the thickness of low conductivity hexadecane, and making the contact tighter. When the hexadecane remelts, the pressure on the graphite flakes is released and the contact area is reduced due to the elastic recovery of graphite flakes and inter-particle repulsion. Therefore, the stress generation during the phase change process is the key reason for the large difference between thermal conductivity at different states.

Although it is well-known that electrical conductivity can be tuned via temperature using the metal-insulator transition [109], temperature regulation of thermal conductivity is not that easy. Our demonstration of reversible regulation in thermal and electrical properties may lead to practical applications of the composites in energy systems.

5. Summary

We have reviewed potential heat conduction mechanisms in nanofluids. Our own experimental studies support cluster formation and percolation as the key factor for the thermal conductivity enhancements. Brownian motion, although cannot be completely ruled out theoretically due to power-law decay, rather than the exponential decay, of the Brownian particle dynamics, is unlikely to make much contribution to thermal conductivity enhancement. Guided by the understanding in heat conduction mechanisms, we have achieved record high thermal conductivity values in graphite suspensions in both oil and water.

The clustering and percolation picture suggests that below the percolation threshold, one may explore the enhanced thermal conductivity of our suspensions in flow systems. Above percolation, viscosity of the fluid will increase rapidly, and the application of our suspensions in fluid situations will be limited. In this regime, stationary applications are more promising. Using phase change to reversibly regulate properties of the suspensions opens up other application possibilities.

Although one should be able to explain the enhanced thermal conductivity of nanofluids by using the clustering and percolation picture, there are also other surprises such as our observation of thermal percolation feature. More fundamentally, the structures of nanoparticle-fluid suspensions are complex, and our understanding of thermal transport in such structures are limited, as the past debate on the thermal conductivity enhancement mechanisms suggests. One can make many substitutions to both the base fluids and the nanoparticles, from inorganic to organic. There is plenty of room to improve the understanding of heat conduction mechanisms in soft materials.

Acknowledgement

The authors wish to thank the funding support from AFOSR FA9550-11-1-0174 (J.J.W. and G.C.), Fundamental Research Funds for the Central Universities (R.T.Z.) and the Program for New Century Excellent Talents in University (R.T.Z). And also thank to Dr. Shuo Chen, Professor Hsien-Ping Feng, Dr. Jae Sik Jin, Professor Yang Shao-horn, and Mr. Ethan Crumlin for fruitful discussions and facility supports, and appreciate Jenny Wang for proofreading the manuscript.

Reference

[1] S.U.S. Choi, D.A. Siginer, H.P. Wang, Developments and Applications of non-Newtonian Flows, New York, 1995, pp. 99-105.

[2] S.K. Das, S.U.S. Choi, W. Yu, T. Pradeep, Nanofluids: Science and Technology, J. Wiley & Sons, Hoboken (N.J.), 2008.

[3] M. Chandrasekar, S. Suresh, Heat Transfer Engineering 30 (2009) 1136-1150.

[4] S. Özerinç, S. Kakaç, A.G. Yazıcıoğlu, Microfluidics and Nanofluidics 8 (2009) 145-170.

[5] J.H. Lee, S.H. Lee, C.J. Choi, S.P. Jang, S.U.S. Choi, International Journal of Micro-Nano Scale Transport 1 (2010) 269 – 322.

[6] V. Trisaksri, S. Wongwises, Renewable and Sustainable Energy Reviews 11 (2007) 512-523.

[7] X.-Q. Wang, A.S. Mujumdar, International Journal of Thermal Sciences 46 (2007) 1-19.

[8] A.S. Ahuja, Journal of Applied Physics 46 (1975) 3408.

[9] J. Maxwell, A Treatise on Electricity and Magnetism, Dover Publications, New York, 1954.

[10] C.-W. Nan, R. Birringer, D.R. Clarke, H. Gleiter, Journal of Applied Physics 81 (1997) 6692.

[11] Y. Benveniste, Journal of Applied Physics 61 (1987) 2840.

[12] D.P.H. Hasselman, L.F. Johnson, Journal of Composite Materials 21 (1987) 508 -515.

[13] D.P.H. Hasselman, K.Y. Donaldson, Journal of Wide Bandgap Materials 7 (2000) 306-318.

[14] J. Happel, AIChE Journal 4 (1958) 197-201.

[15] R.L. Hamilton, O.K. Crosser, Industrial & Engineering Chemistry Fundamentals 1 (1962) 187-191.

[16] H. Masuda, A. Ebata, K. Teramae, N. Hishinuma, Netsu Bussei 7 (1993) 227-233.

[17] W. Yu, S.U.S. Choi, Journal of Nanoparticle Research 5 (2003) 167-171.

[18] P. Keblinski, S.R. Phillpot, S.U.S. Choi, J.A. Eastman, International Journal of Heat and Mass Transfer 45 (2002) 855-863.

[19] J.W. Gao, R.T. Zheng, H. Ohtani, D.S. Zhu, G. Chen, Nano Letters 9 (2009) 4128-4132.

[20] S.P. Jang, S.U.S. Choi, Journal of Heat Transfer 129 (2007) 617-623.

[21] D.P. Kulkarni, R.S. Vajjha, D.K. Das, D. Oliva, Applied Thermal Engineering 28 (2008) 1774-1781.

[22] X.-F. Yang, Z.-H. Liu, Nanoscale Research Letters 6 (2011) 494.

[23] T. Parametthanuwat, S. Rittidech, A. Pattiya, Y. Ding, S. Witharana, Nanoscale Research Letters 6 (2011) 315.

[24] S.A. Putnam, D.G. Cahill, P.V. Braun, Z. Ge, R.G. Shimmin, Journal of Applied Physics 99 (2006) 084308.

[25] X. Zhang, H. Gu, M. Fujii, Journal of Applied Physics 100 (2006) 044325.

[26] J. Eapen, W.C. Williams, J. Buongiorno, L.-wen Hu, S. Yip, R. Rusconi, R. Piazza, Physical Review Letters 99 (2007) 095901.

[27] E.V. Timofeeva, A.N. Gavrilov, J.M. McCloskey, Y.V. Tolmachev, S. Sprunt, L.M. Lopatina, J.V. Selinger, Physical Review E 76 (2007) 061203.

[28] J. Buongiorno, D.C. Venerus, N. Prabhat, T. McKrell, J. Townsend, R. Christianson, Y.V. Tolmachev, P. Keblinski, L.-wen Hu, J.L. Alvarado, I.C. Bang, S.W. Bishnoi, M. Bonetti, F. Botz, A. Cecere, Y. Chang, G. Chen, H. Chen, S.J. Chung, M.K. Chyu, S.K. Das, R. Di Paola, Y. Ding, F. Dubois, G. Dzido, J. Eapen, W. Escher, D. Funfschilling, Q. Galand, J. Gao, P.E.

Gharagozloo, K.E. Goodson, J.G. Gutierrez, H. Hong, M. Horton, K.S. Hwang, C.S. Iorio, S.P. Jang, A.B. Jarzebski, Y. Jiang, L. Jin, S. Kabelac, A. Kamath, M.A. Kedzierski, L.G. Kieng, C. Kim, J.-H. Kim, S. Kim, S.H. Lee, K.C. Leong, I. Manna, B. Michel, R. Ni, H.E. Patel, J. Philip, D. Poulikakos, C. Reynaud, R. Savino, P.K. Singh, P. Song, T. Sundararajan, E. Timofeeva, T. Tritcak, A.N. Turanov, S. Van Vaerenbergh, D. Wen, S. Witharana, C. Yang, W.-H. Yeh, X.-Z. Zhao, S.-Q. Zhou, Journal of Applied Physics 106 (2009) 094312.

[29] P. Keblinski, R. Prasher, J. Eapen, Journal of Nanoparticle Research 10 (2008) 1089-1097.

[30] L. Xue, P. Keblinski, S.. Phillpot, S.U.-S. Choi, J. Eastman, International Journal of Heat and Mass Transfer 47 (2004) 4277-4284.

[31] A. Schmidt, M. Chiesa, X. Chen, G. Chen, Review of Scientific Instruments 79 (2008) 064902.

[32] J. Garg, B. Poudel, M. Chiesa, J.B. Gordon, J.J. Ma, J.B. Wang, Z.F. Ren, Y.T. Kang, H. Ohtani, J. Nanda, G.H. McKinley, G. Chen, Journal of Applied Physics 103 (2008) 074301.

[33] R.T. Zheng, J.W. Gao, J.J. Wang, G. Chen, Nature Communications 2 (2011) 289.

[34] A.J. Schmidt, J.D. Alper, M. Chiesa, G. Chen, S.K. Das, K. Hamad-Schifferli, The Journal of Physical Chemistry C 112 (2008) 13320-13323.

[35] M. Chiesa, J. Garg, Y. Kang, G. Chen, Colloids and Surfaces A: Physicochemical and Engineering Aspects 326 (2008) 67–72.

[36] A.J. Schmidt, M. Chiesa, D.H. Torchinsky, J.A. Johnson, K.A. Nelson, G. Chen, Journal of Applied Physics 103 (2008) 083529.

[37] J.J. Ma, Thermal Conductivity of Fluids Containing Suspension of Nanometer-Sized Particles, Massachusetts Institute of Technology, 2006.

[38] R.T. Zheng, J.W. Gao, G. Chen, Graphite Microfluids, Patent pending.

[39] R.T. Zheng, J.W. Gao, G. Chen, Thermal And/or Electrical Conductivity Controls in Suspensions, Patent pending.

[40] W. Yu, H. Xie, Journal of Nanomaterials 2012 (2012) 1-17.

[41] W. Yu, D.M. France, S.U.S. Choi, J.L. Routbort, Argonne National Laboratory Technical Report (2007).

[42] W. Yu, D.M. France, J.L. Routbort, S.U.S. Choi, Heat Transfer Engineering 29 (2008) 432-460.

[43] J.A. Eastman, S.R. Phillpot, S.U.S. Choi, P. Keblinski, Annual Review of Materials Research 34 (2004) 219-246.

[44] R. Prasher, P.E. Phelan, P. Bhattacharya, Nano Letters 6 (2006) 1529-1534.

[45] N.R. Karthikeyan, J. Philip, B. Raj, Materials Chemistry and Physics 109 (2008) 50-55.

[46] J. Philip, P.D. Shima, B. Raj, Nanotechnology 19 (2008) 305706.

[47] X. Jie, Y. Bo-Ming, Y. Mei-Juan, Chinese Physics Letters 23 (2006) 2819-2822.

[48] H. Zhu, C. Zhang, S. Liu, Y. Tang, Y. Yin, Applied Physics Letters 89 (2006) 023123.

[49] S. Shaikh, K. Lafdi, R. Ponnappan, Journal of Applied Physics 101 (2007) 064302.

[50] M.J. Assael, C.-F. Chen, I. Metaxa, W.A. Wakeham, International Journal of Thermophysics 25 (2004) 971-985.

[51] T.T. Baby, S. Ramaprabhu, Nanoscale Research Letters 6 (2011) 289.

[52] G. Chen, Nanoscale Energy Transport and Conversion a Parallel Treatment of Electrons, Molecules, Phonons, and Photons, Oxford University Press, New York, Oxford, 2005.

[53] K. Esfarjani, G. Chen, H.T. Stokes, Physical Review B 84 (2011) 085204.

[54] A.S. Henry, G. Chen, Journal of Computational and Theoretical Nanoscience 5 (2008) 141-152.

[55] C.L. Tien, G. Chen, Journal of Heat Transfer 116 (1994) 799-807.

[56] P. Kim, L. Shi, A. Majumdar, P.L. McEuen, Physical Review Letters 87 (2001) 215502.

[57] S. Ghosh, W. Bao, D.L. Nika, S. Subrina, E.P. Pokatilov, C.N. Lau, A.A. Balandin, Nature Materials 9 (2010) 555-558.

[58] S. Berber, Y.-K. Kwon, D. Tománek, Physical Review Letters 84 (2000) 4613-4616.

[59] J.H. Seol, I. Jo, A.L. Moore, L. Lindsay, Z.H. Aitken, M.T. Pettes, X. Li, Z. Yao, R. Huang, D. Broido, N. Mingo, R.S. Ruoff, L. Shi, Science 328 (2010) 213 -216.

[60] G. Kikugawa, T. Ohara, T. Kawaguchi, E. Torigoe, Y. Hagiwara, Y. Matsumoto, The Journal of Chemical Physics 130 (2009) 074706.

[61] D. Viswanath, M.B. Rao, Journal of Physics D: Applied Physics 3 (1970) 1444.

[62] D. Bertolini, A. Tani, Physical Review E 56 (1997) 4135-4151.

[63] E.T. Swartz, R.O. Pohl, Reviews of Modern Physics 61 (1989) 605-668.

[64] W.A. Little, Canadian Journal of Physics 37 (1959) 334.

[65] P.L. Kapitza, Physical Review 60 (1941) 354-355.

[66] R.E. Peterson, A.C. Anderson, Physics Letters A 40 (1972) 317-319.

[67] R. Prasher, Applied Physics Letters 94 (2009) 041905.

[68] Z. Ge, D.G. Cahill, P.V. Braun, Physical Review Letters 96 (2006) 186101.

[69] Z. Ge, D.G. Cahill, P.V. Braun, J. Phys. Chem. B 108 (2004) 18870-18875.

[70] S.T. Huxtable, D.G. Cahill, S. Shenogin, L. Xue, R. Ozisik, P. Barone, M. Usrey, M.S. Strano, G. Siddons, M. Shim, P. Keblinski, Nature Materials 2 (2003) 731-734.

[71] O.M. Wilson, X. Hu, D.G. Cahill, P.V. Braun, Physical Review B 66 (2002) 224301.

[72] S.P. Jang, S.U.S. Choi, Applied Physics Letters 84 (2004) 4316.

[73] R. Prasher, P. Bhattacharya, P.E. Phelan, Physical Review Letters 94 (2005) 025901.

[74] A. Einstein, Investigations on the Theory of the Brownian Movement, Dover, [New York], 1956.

[75] P. Keblinski, D.G. Cahill, Physical Review Letters 95 (2005) 209401.

[76] P. Bhattacharya, Journal of Applied Physics 95 (2004) 6492.

[77] J. Wang, G. Chen, Z. Zhang, in:, Proceedings of 2005 ASME Summer Heat Transfer Conference, 2005.

[78] B.J. Alder, T.E. Wainwright, Physical Review Letters 18 (1967) 988-990.

[79] Y. Xuan, Q. Li, W. Hu, AIChE Journal 49 (2003) 1038-1043.

[80] B. Yang, Journal of Heat Transfer 130 (2008) 042408-5.

[81] W. Evans, J. Fish, P. Keblinski, Applied Physics Letters 88 (2006) 093116.

[82] S. Kumar Das, N. Putra, P. Thiesen, W. Roetzel, Journal of Heat Transfer 125 (2003) 567-574.

[83] A. Turgut, I. Tavman, M. Chirtoc, H.P. Schuchmann, C. Sauter, S. Tavman, International Journal of Thermophysics 30 (2009) 1213-1226.

[84] P.J. Lu, E. Zaccarelli, F. Ciulla, A.B. Schofield, F. Sciortino, D.A. Weitz, Nature 453 (2008) 499-503.

[85] P.J. Lu, J.C. Conrad, H.M. Wyss, A.B. Schofield, D.A. Weitz, Physical Review Letters 96 (2006) 028306.

[86] E. Zaccarelli, P. Lu, F. Ciulla, D. Weitz, F. Sciortino, Journal of Physics: Condensed Matter 20 (2008) 494242.

[87] A.J. Minnich, J.A. Johnson, A.J. Schmidt, K. Esfarjani, M.S. Dresselhaus, K.A. Nelson, G. Chen, Physical Review Letters 107 (2011) 095901.

[88] G. Chen, Journal of Heat Transfer 119 (1997) 220-229.

[89] H.E. Patel, V.R.R. Kumar, T. Sundararajan, T. Pradeep, S.K. Das, Physical Review Letters 93 (2004) 144301.

[90] J. Buongiorno, Journal of Heat Transfer 128 (2006) 240-250.

[91] J. Koo, C. Kleinstreuer, International Communications in Heat and Mass Transfer 32 (2005) 1111-1118.

[92] G. Domingues, S. Volz, K. Joulain, J.-J. Greffet, Physical Review Letters 94 (2005) 085901.

[93] S. Shen, A. Narayanaswamy, G. Chen, Nano Letters 9 (2009) 2909-2913.

[94] D. Venerus, J. Buongiorno, R. Christianson, J. Townsend, I. Bang, G. Chen, S. Chung, M. Chyu, H. Chen, Y. Ding, others, Applied Rheology 20 (2010).

[95] M. Dresselhaus, Graphite Fibers and Filaments, Springer-Verlag, Berlin, New York, 1988.

[96] K. Kalaitzidou, H. Fukushima, L.T. Drzal, Composites Science and Technology 67 (2007) 2045-2051.

[97] K. Kalaitzidou, H. Fukushima, L.T. Drzal, Composites Part A 38 (2007) 1675-1682.

[98] S. Stankovich, D.A. Dikin, G.H.B. Dommett, K.M. Kohlhaas, E.J. Zimney, E.A. Stach, R.D. Piner, S.T. Nguyen, R.S. Ruoff, Nature 442 (2006) 282-286.

[99] Yasmin, J. Luo, I. Daniel, Composites Science and Technology 66 (2006) 1182-1189.

[100] R.T.. Zheng, J.W.. Gao, J.J.. Wang, Nano Letters (accepted).

[101] S.U.S. Choi, Z.G. Zhang, W. Yu, F.E. Lockwood, E.A. Grulke, Applied Physics Letters 79 (2001) 2252.

[102] H. Zhu, C. Zhang, Y. Tang, J. Wang, B. Ren, Y. Yin, Carbon 45 (2007) 203-228.

[103] M.J. Biercuk, M.C. Llaguno, M. Radosavljevic, J.K. Hyun, A.T. Johnson, J.E. Fischer, Applied Physics Letters 80 (2002) 2767.

[104] N. Shenogina, S. Shenogin, L. Xue, P. Keblinski, Applied Physics Letters 87 (2005) 133106-133106-3.

[105] K.-Y. Chun, Y. Oh, J. Rho, J.-H. Ahn, Y.-J. Kim, H.R. Choi, S. Baik, Nature Nanotechnology 5 (2010) 853-857.

[106] S. Deville, E. Saiz, R.K. Nalla, A.P. Tomsia, Science 311 (2006) 515 -518.

[107] K.M. Golden, S.F. Ackley, V.I. Lytle, Science 282 (1998) 2238 -2241.

[108] D. Porter, Phase Transformations in Metals and Alloys, 2nd ed., Nelson Thornes, Cheltenham, 2001.

[109] R.G. Moore, J. Zhang, V.B. Nascimento, R. Jin, J. Guo, G.T. Wang, Z. Fang, D. Mandrus, E.W. Plummer, Science 318 (2007) 615 -619.